



# Enhancement of Mechanical Properties in FRP-Reinforced Glulam Column-Beam Connections: A FEM Approach



Yasemin Şimşek Türker<sup>✉</sup>, Şemsettin Kilinçarslan<sup>\*</sup><sup>✉</sup>, Mehmet Avcar<sup>✉</sup>

Department of Civil Engineering, University of Suleyman Demirel, 32000 Isparta, Turkey

\* Correspondence: Şemsettin Kilinçarslan (mehmetavcar@sdu.edu.tr)

Received: 12-22-2023

Revised: 02-02-2024

Accepted: 02-10-2024

**Citation:** Y. Ş. Türker, Ş. Kilinçarslan, and M. Avcar, “Enhancement of mechanical properties in FRP-reinforced glulam column-beam connections: A FEM approach,” *GeoStruct. Innov.*, vol. 2, no. 1, pp. 10–20, 2024. <https://doi.org/10.56578/gsi020102>.



© 2024 by the authors. Published by Acadlore Publishing Services Limited, Hong Kong. This article is available for free download and can be reused and cited, provided that the original published version is credited, under the CC BY 4.0 license.

**Abstract:** Glued laminated timber (glulam), a composite material fabricated by bonding multiple wood layers, is engineered to support specific loads, offering reduced product variability and diminished sensitivity to inherent wood characteristics, such as knots. This technology facilitates a wide array of architectural designs, rendering it a popular choice for load-bearing elements across diverse construction projects, including residential structures, storage facilities, and pedestrian overpasses. Over time, exposure to various environmental conditions leads to the degradation of these structural components, necessitating periodic reinforcement to maintain their strength properties. Recent advancements have seen the adoption of fiber-reinforced polymer (FRP) for the reinforcement of columns and beams, a departure from traditional strengthening methods. This study focuses on the connection of column-beam joints using an array of steel fasteners, subsequently reinforced with FRP. Rotational tests were conducted on these fabricated connections, followed by a comprehensive analysis using the finite element method (FEM). Results indicate that connections reinforced with FRP exhibit a significant enhancement in load-carrying capacity, energy dissipation, and stiffness compared to their unreinforced counterparts. Specifically, the load-carrying capacity showed an increase of 25–39%, energy dissipation capacity augmented by 64–69%, and stiffness values rose by 2–7%. These findings underscore the efficacy of FRP reinforcement in improving the structural integrity and performance of glulam column-beam connections, offering valuable insights for the design and renovation of wood-based construction elements.

**Keywords:** Composite materials; Reinforcement; Fiber-reinforced polymer; Wood structures; Finite element method

## 1 Introduction

Due to inherent flaws leading to early fragile failure in the tension area, along with their comparatively lower bending stiffness relative to steel or reinforced concrete beams of similar cross-sections, wooden beams are not frequently utilized [1–3]. Different composite materials can be used to enhance the material properties of wood materials, as composite materials are especially used as carrier elements in wooden structures, such as glued laminated timber (glulam) [4–8].

Glulam is a widely used composite material that improves the strength properties of wooden materials. Additionally, it can be produced in a variety of shapes and lengths from a variety of tree species [9–11]. The term “glulam” pertains to a material formed by adhering the edges and surfaces of wooden panels, aligning the wood grain parallel to the piece’s axis. Lengthy panels are formed by longitudinally combining planks, attaching them face-to-face and edge-to-edge to obtain the required dimensions [12–16]. Furthermore, these panels can be flexed to yield curved forms during the gluing process. The mentioned aspects collectively offer a diverse array of design possibilities, primarily restricted by the costs associated with production and application [17–20].

A variety of techniques have been used to increase the flexural performance of both glulam and solid timber beams through the inclusion of reinforcements to optimize the use of lower-grade timber, decrease beam depth, and improve reliability. Metallic reinforcements, which include steel bars, steel strips, steel or aluminum plates, and even high-strength steel cords, are among the most often used reinforcing materials for timber beams [21–27]. This kind of metal reinforcement was common in the early stages, especially in the 1960s, because the use of steel reinforcement in timber construction offers both structural efficiency and cost-effectiveness [28–36].

In recent times, FRP has been utilized in a variety of forms, such as sheets, plates, strips, and bars, to provide structural reinforcement for timber beams [37–42]. Furthermore, as a sustainable alternative, natural fibers have been employed to reinforce timber construction [43, 44]. Systems with great mechanical performance and low weight are usually the outcome of using FRP or natural fiber materials as reinforcements. Besides, the improved corrosion resistance of FRP reinforcement over traditional steel reinforcing materials is another noteworthy benefit [45, 46].

Remarkably, studies have been conducted to reinforce timber beams using pre-stressed steel, or FRP, in order to improve their flexural behavior [47–50]. The results showed a significant increase in flexural strength due to the complete use of both the reinforcement and wood components. Furthermore, the flexural stiffness was significantly increased as a result of the precamber developed in the flexural members. The bulk of previous research has shown that the addition of these reinforcing materials has a substantially favorable influence on the flexural behavior of timber beams [51–54].

The goal of this study is to improve the resilience of column-beam joints, which are a particularly vulnerable location in structures during earthquakes, using lightweight, non-corrosive, and flexible FRP. In order to achieve this goal, combinations of WV90080 and ALUMIDI 160 and WV90110 and ALUMIDI 200 fasteners are used to construct glulam column-beam junctions, providing two examples for each kind of connection. Four of the eight fabricated samples are left uncovered, while the other four are wrapped. Following development as part of this investigation, the column-beam joint samples were put through a load-displacement test per the experimental setup. The ANSYS finite element software is used to simulate column-beam joints after the experiments.

## 2 Methodology

The first sample consisted of a column component of 1000 mm in length and 120×120 mm (C12) in cross-section, combined with a beam component that is 1500 mm in length and 120×240 mm in cross-section. Regarding the second sample, the column member has dimensions of 140×140 mm (C14) in cross-section and 1000 mm in length, while the beam member has 140×280 mm in cross-section and 1500 mm in length. The glulam columns and beams are supplied by Nasreddin Forest Products (Naswood), located in Antalya. During the manufacturing process, melamine formaldehyde glue is used to laminate spruce timbers with a humidity level of 11–12%. After the column and beam bearing parts are fabricated, the samples are joined together using the ALUMIDI series, which is characteristic of wooden structural joints, and frequently used angle brackets. WV90080 (W8) and ALUMIDI 160 (A16) and WV90110 (W1) and ALUMIDI 200 (A20) from the Rothoblass catalog are utilized for the samples with dimensions of 120×120-120×240 mm and 140×140-140×280 mm, respectively. Eight samples are examined in total, generating two from each sample [55], and the codes for the generated samples are listed in Table 1.

A carbon fiber-reinforced polymer composite fabric with the code MasterBrace FIB 600/100 CFS is used to reinforce the beams. The following steps are applied in the FRP fabric reinforcing process: After carefully cleaning the material's surface, a primer is applied, then the glue is carefully used within 1-1.5 hours; and lastly, fiber polymer textiles are carefully wound onto the surface covered with adhesive. The 300/50 CFS 300 g/m<sup>2</sup> weight fabrics based on carbon have been supplied from ÜNAL TEKNİK® Practice Construction Industry and Trade Ltd. Sti. for use in the present study. Five steps are involved in winding the FRP fabric around the column-beam joints, and each step involves three layers of wrapping. The load-displacement test was executed within a frame constructed with sufficiently rigid steel carrier elements. The experiments followed a displacement control method, subjecting the samples to cyclic loading from the beam end regions. Across all experiments, a total of 26 loading steps are implemented, with each step undergoing 4 repetitions.

Figure 1 provides a visual representation of the lines illustrating the area and slopes used in the calculations for total energy dissipation capacity and stiffness [55].

**Table 1.** Characteristics of column beam connections

No.	Size of Column (mm)	Size of Beam (mm)	Type of Connection	Status of Reinforcement	Code of Sample
1	120 × 120	120 × 240	ALUMIDI-160L	-	C12-A16-UR
2	120 × 120	120 × 240	ALUMIDI-160L	+	C12-A16-R
3	120 × 120	120 × 240	WVS 90080	-	C12-W8-UR
4	120 × 120	120 × 240	WVS 90080	+	C12-W8-R
5	140 × 140	140 × 280	WVS 90110	-	C14-W1-UR
6	140 × 140	140 × 280	WVS 90110	+	C14-W1-R
7	140 × 140	140 × 280	ALUMIDI-200L	-	C14-A20-UR
8	140 × 140	140 × 280	ALUMIDI-200L	+	C14-A20-R

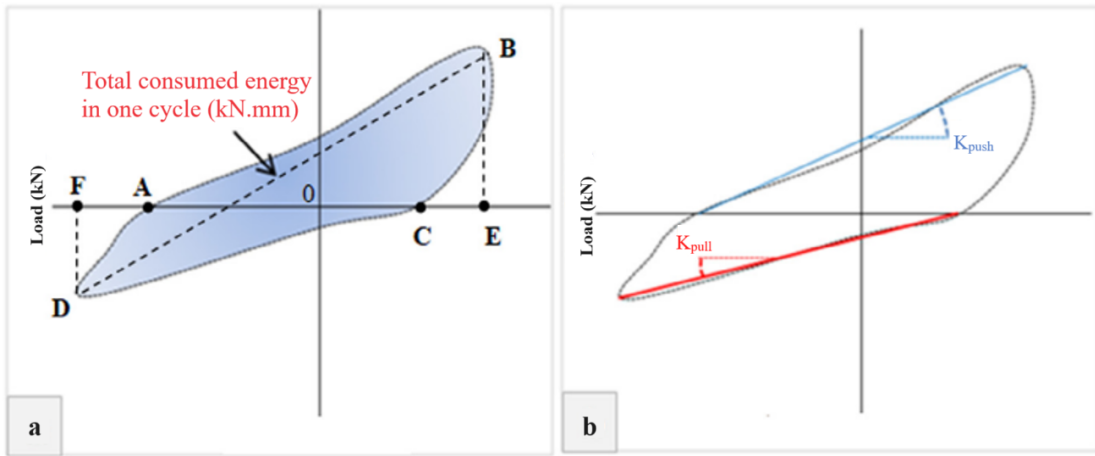


**Figure 1.** a) energy dissipation capacity; b) stiffness

After conducting the computations, the study determined both the energy dissipation capability per cycle and the cumulative energy dissipation by the conclusion of the experiment. Furthermore, the stiffness metrics in both the push and pull orientations were assessed for each cycle.

The numerical simulation utilizes the ANSYS 18.1 Standard Solver in combination with the FEM. Models are created to represent both unenhanced and strengthened column-beam connections, guaranteeing that their shapes and applied loads correspond to those tested in experiments. The terminal constraints, which limit vertical displacement, are replicated using pinned and roller supports. A 25-mm square mesh is employed in the modeling phase. It is assumed that there exists an impeccable bond at the interface between laminated timbers and FRP, and the appropriate boundary conditions are applied to the column-beam connections model to imitate the constraints of a simply supported system.

The timber section makes use of the SOLID45 element, which is tailored for three-dimensional modeling of solid structures and includes eight nodes, each endowed with three degrees of freedom (along the three axes). SOLID45 incorporates abilities like plasticity and stress-induced stiffening, accounting for substantial deflections and strains. Nevertheless, providing a precise portrayal of the complex anisotropic nature of timber is deemed impractical. Instead, the software requires the elastic characteristics of the timber to be entered in an orthogonal format for behavioral simulation.

The SOLID65 element, equipped with eight nodes and allowing three degrees of freedom at each node (in the x, y, and z directions), is utilized to replicate the behavior of FRP. This choice is based on its effectiveness in predicting tension cracking and compression crushing. It finds widespread application in simulating reinforced composites like FRP, concrete, and geological rocks. FRP material is thought to have linear elastic characteristics with brittle failure because of the little plastic deformation it experiences. The FRP materials are simplified by modeling them to have uniaxial linear isotropic behavior. With these considerations and assumptions, the SOLID65 element can accurately replicate their behavior. Since previous research has established a seamless connection between laminations in glulam beams, each material attribute is taken into account. The melamine formaldehyde adhesive layer is removed from the FEM model due to its extremely thin nature. Additionally, based on the excellent bonding shown during testing, the connections between epoxy and FRP and epoxy and timber are expected to be perfect. All elements were modeled as a solid FEM featuring eight nodes and reduced integration. A finer mesh is applied to the laminations near the FRP reinforcement, where stress is transmitted from the FRP plate to the glulam. To represent the bonding between wood laminations and the interfaces of wood, epoxy, and FRP, a “tie constraint” was implemented.

### 3 Results

The modeled column-beam connections were analyzed in push and pull directions. ANSYS program images of the analyzed samples are given in Figure 2 to Figure 9.

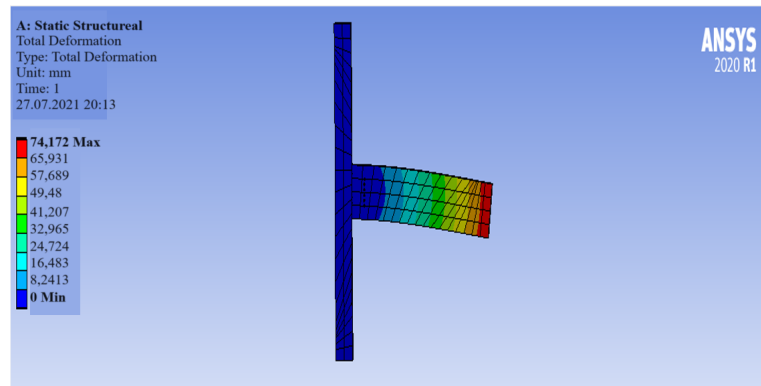
The data in Table 2 presents the average (average of push and pull directions) maximum load-carrying capacity, energy consumption capacity, and stiffness value obtained from the load-displacement data.

The highest load-carrying capacity (13.66 kN) is obtained for the column beam with the code C14-W1-R, while the lowest one (06.59 kN) is found for the column beam with the code C12-A16-UR. The load-carrying capacity of the column-beam connection with the code C12-A16-R is 27.74% higher than that of the code C12-A16-UR. The load-carrying capacity of the C12-W8-R-coded column-beam connection is 30.76% higher than that of the C12-W8-UR-coded beam. The load-carrying capacity of the C14-W1-R-coded column-beam connection is 25.84%

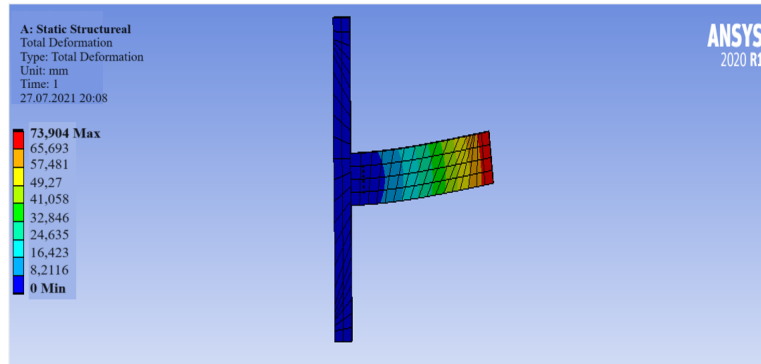
higher than that of the C14-W1-UR-coded beam. The C14-A20-R-coded column-beam connection is 39.11% higher than the C14-A20-UR-coded beam. When energy dissipation capacities were examined, column-beam connections coded C12-A16-UR obtained the lowest value (402 kN.mm). The highest energy dissipation capacity value (2741 kN.mm) was obtained in the column-beam connection coded C14-W1-R. The lowest energy dissipation capacity value (402 kN.mm) was obtained in the beam-coded C12-A16-UR. The energy absorption capacity of reinforced column-beam connections increased by approximately 64-69%. When the stiffness values were examined, the highest stiffness value (1200 kN/mm) was obtained in column-beam connections coded C14-W1-R, and the lowest value (230 kN/mm) was obtained in column-beam connections coded C12-A16-UR. When the numerical and experimental analysis results were compared, it was determined that the load-carrying capacity, energy consumption amount, and stiffness values gave similar results. It was determined that there was a maximum difference of 6% in load-carrying capacity values, 9% in energy consumption capacity values, and 0.75% in stiffness values.

**Table 2.** Data obtained as a result of the experiments and ANSYS analysis

Sample Code	Load Carrying Capacity (kN)	Energy Consumption (kN.mm)	Stiffness (kN/mm)	Load Carrying Capacity (kN)	Energy Consumption (kN.mm)	Stiffness (kN/mm)
C12-A16-UR	06.59	402	230	05.62	416	232
C12-A16-R	09.12	1120	275	08.15	1295	281
C12-W8-UR	07.36	692	350	6.94	704	347
C12-W8-R	10.63	1546	675	10.61	1456	660
C14-W1-UR	10.13	868	410	09.43	861	416
C14-W1-R	13.66	2741	1200	14.02	2694	1191
C14-A20-UR	07.27	546	405	07.81	528	395
C14-A20-R	11.94	1236	1100	11.92	1362	1119

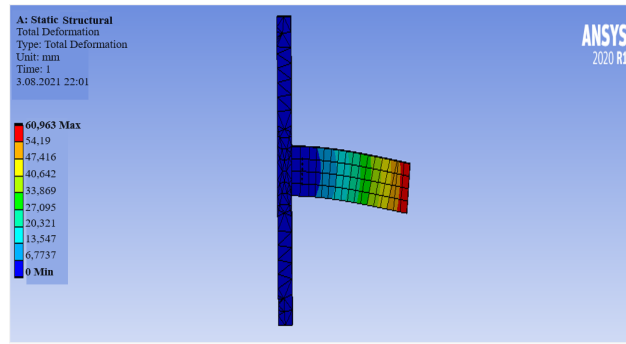


(a)

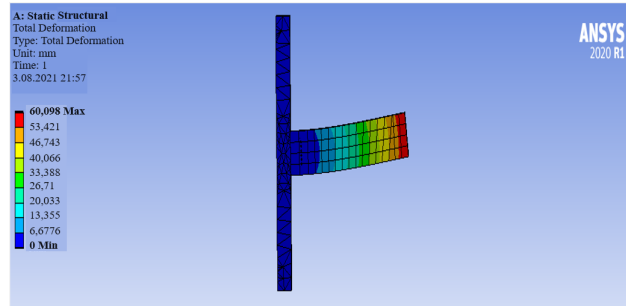


(b)

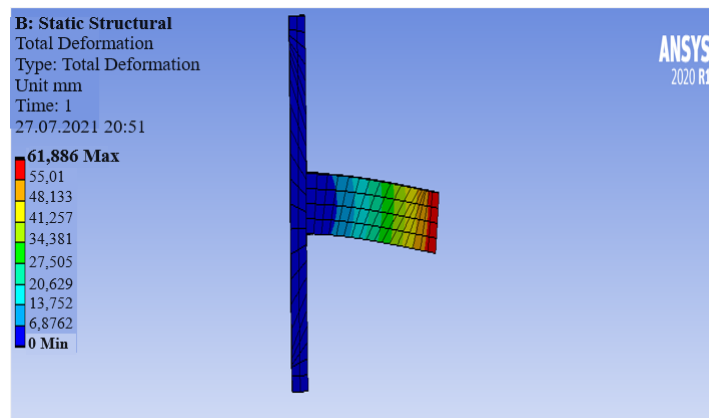
**Figure 2.** Analysis of the sample coded C12-A16-UR in the direction of push and pull



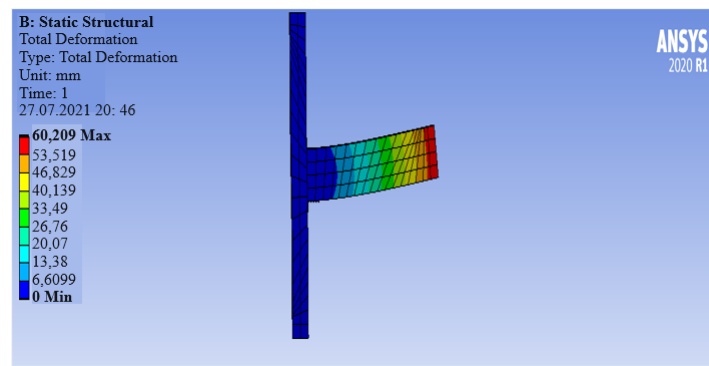
(a)



(b)

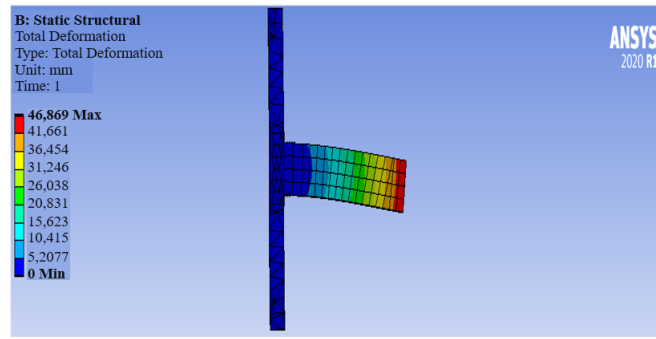
**Figure 3.** Analysis of the sample coded C12-A16-R in the direction of push and pull

(a)

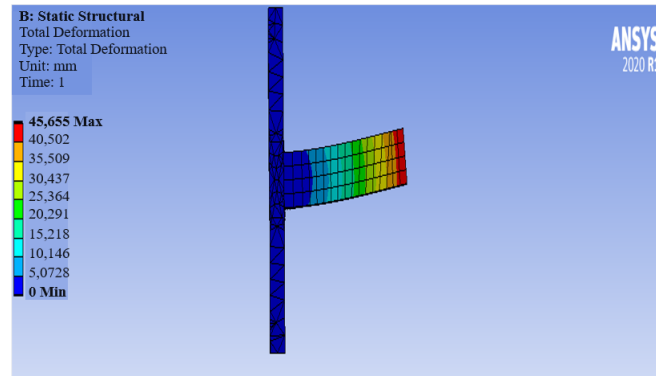


(b)

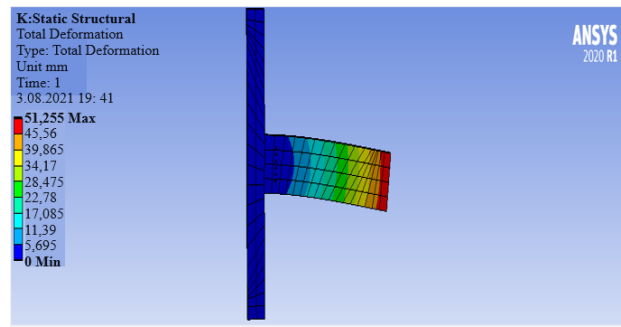
**Figure 4.** Analysis of the sample coded C12-W8-UR in the direction of push and pull



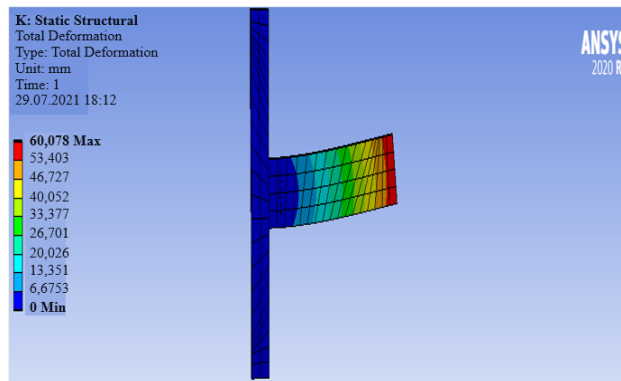
(a)



(b)

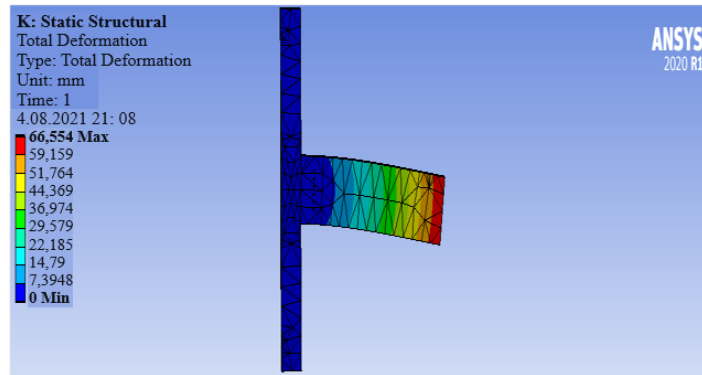
**Figure 5.** Analysis of the sample coded C12-W8-R in the direction of push and pull

(a)

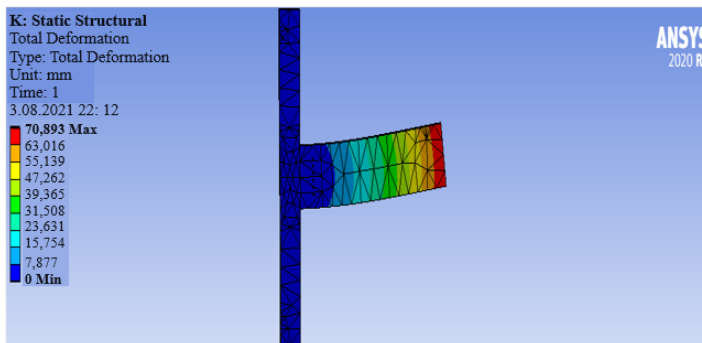


(b)

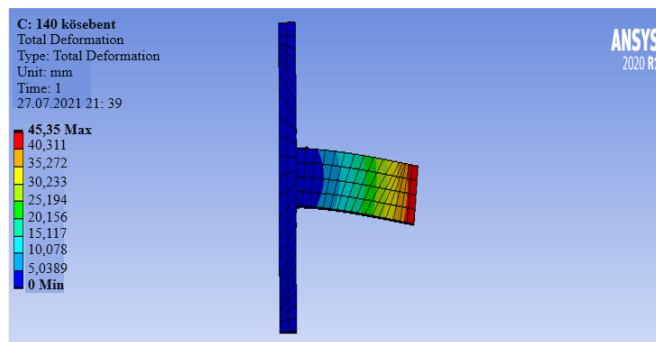
**Figure 6.** Analysis of the sample coded C14-A20-UR in the direction of push and pull



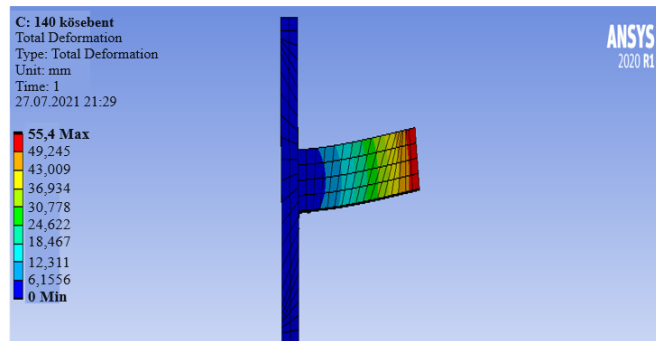
(a)



(b)

**Figure 7.** Analysis of the sample coded C14-A20-R in the direction of push and pull

(a)



(b)

**Figure 8.** Analysis of the sample coded C14-W1-UR in the direction of push and pull

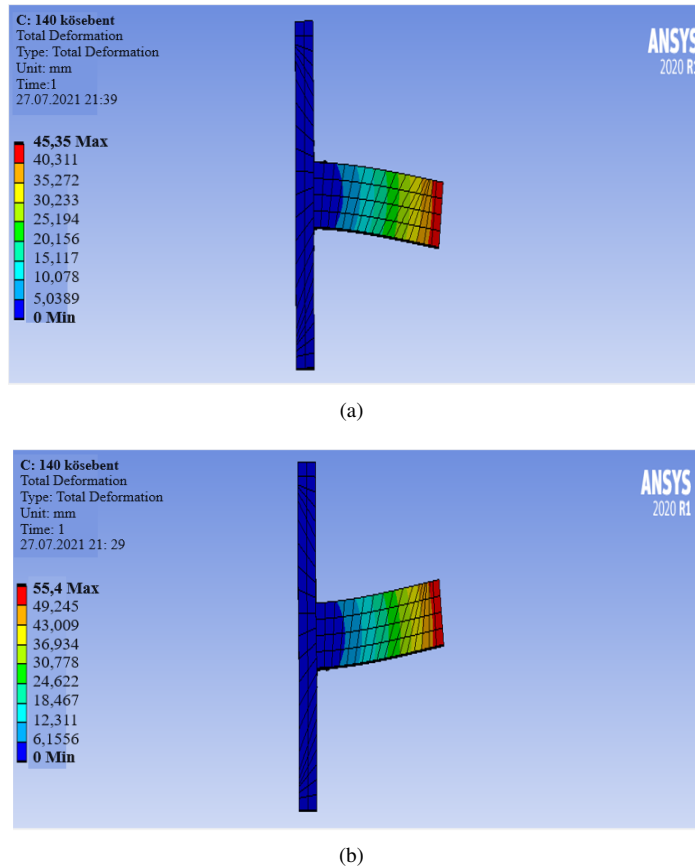


**Figure 9.** Analysis of the sample coded C14-W1-R in the direction of push and pull

#### 4 Conclusion

In the present research, the rotational behavior properties of FRP-reinforced column-beam connections were investigated experimentally and numerically. The highest load-carrying capacity, energy dissipation, and stiffness values belong to reinforced column-beam connections. The lowest load-carrying capacity, energy dissipation values, and stiffness values refer to unreinforced column-beam connections. With the reinforcement of column-beam connections, the load carrying increased by 25-39%, the energy dissipation capacity increased by 64-69%, and stiffness values increased by 2-7%. Additionally, when examined in terms of size, as the cross-section dimensions increased, the rotational properties of the column-beam connections increased.

Upon comparing the numerical and experimental analysis outcomes, it was observed that the load-carrying capacity, energy consumption, and stiffness values exhibited comparable results. Specifically, there was a maximum disparity of 6% in load-bearing capacity, 9% in energy consumption, and 0.75% in stiffness. Numerical analyses and experimental studies gave similar results. It has been observed that column-beam joints reinforced with polymer fabrics made stronger by using fiber can be simulated with the FEM program.

#### Data Availability

The data used to support the findings of this study are available from the corresponding author upon request.

#### Conflicts of Interest

The authors declare that they have no conflicts of interest.

#### References

- [1] H. T. Sahin, M. B. Arslan, S. Korkut, and C. Sahin, “Colour changes of heat-treated woods of red-bud maple, european hophornbeam and oak,” *Color Res. Appl.*, vol. 36, no. 6, pp. 462–466, 2011. <https://doi.org/10.1002/COL.20634>
- [2] C. K. Sahin, M. Topay, and A. A. Var, “A study on suitability of some wood species for landscape applications: Surface color, hardness and roughness changes at outdoor conditions,” *Wood Res.*, vol. 65, no. 3, pp. 395–404, 2020. <https://doi.org/10.37763/WR.1336-4561/65.3.395404>

- [3] H. Johnsson, T. Blanksvärd, and A. Carolin, “Glulam members strengthened by carbon fibre reinforcement,” *Mater. Struct.*, vol. 40, no. 1, pp. 47–56, 2007. [https://doi.org/10.1617/S11527-006-9119-7/METRICS](https://doi.org/10.1617/S11527-006-9119-7)
- [4] C. A. Issa and Z. Kmeid, “Advanced wood engineering: Glulam beams,” *Constr. Build. Mater.*, vol. 19, no. 2, pp. 99–106, 2005. <https://doi.org/10.1016/j.conbuildmat.2004.05.013>
- [5] T. Toratti, S. Schnabl, and G. Turk, “Reliability analysis of a glulam beam,” *Struct. Saf.*, vol. 29, no. 4, pp. 279–293, 2007. <https://doi.org/10.1016/j.strusafe.2006.07.011>
- [6] B. Anshari, Z. W. Guan, and Q. Y. Wang, “Modelling of glulam beams pre-stressed by compressed wood,” *Compos. Struct.*, vol. 165, pp. 160–170, 2017. <https://doi.org/10.1016/j.compstruct.2017.01.028>
- [7] R. O. Foschi and J. D. Barrett, “Glued-laminated beam strength: A model,” *J. Struct. Div.*, vol. 106, no. 8, pp. 1735–1754, 1980.
- [8] T. Smith, F. C. Ponzo, A. Di Cesare, S. Pampanin, D. Carradine, A. H. Buchanan, and D. Nigro, “Post-tensioned glulam beam-column joints with advanced damping systems: Testing and numerical analysis,” *J. Earthq. Eng.*, vol. 18, no. 1, pp. 147–167, 2014. <https://doi.org/10.1080/13632469.2013.835291>
- [9] Z. W. Guan, P. D. Rodd, and D. J. Pope, “Study of glulam beams pre-stressed with pultruded grp,” *Comput. Struct.*, vol. 83, no. 28-30, pp. 2476–2487, 2005. <https://doi.org/10.1016/j.compstruc.2005.03.021>
- [10] I. Glišović, M. Pavlović, B. Stevanović, and M. Todorović, “Numerical analysis of glulam beams reinforced with cfrp plates,” *J. Civ. Eng. Manag.*, vol. 23, no. 7, pp. 868–879, 2017. <https://doi.org/10.3846/13923730.2017.1341953>
- [11] M. Uzel, A. Togay, Ö. Anil, and C. Söyütlü, “Experimental investigation of flexural behavior of glulam beams reinforced with different bonding surface materials,” *Constr. Build. Mater.*, vol. 158, pp. 149–163, 2018. <https://doi.org/10.1016/j.conbuildmat.2017.10.033>
- [12] M. Wang, X. Song, X. Gu, and J. Tang, “Bolted glulam beam-column connections under different combinations of shear and bending,” *Eng. Struct.*, vol. 181, pp. 281–292, 2019. <https://doi.org/10.1016/j.engstruct.2018.12.024>
- [13] W. G. Davids, H. J. Dagher, and J. M. Breton, “Modeling creep deformations of frp-reinforced glulam beams,” *Wood Fiber Sci.*, vol. 32, no. 4, pp. 426–441, 2000.
- [14] M. He, Y. Wang, Z. Li, L. Zhou, Y. Tong, and X. Sun, “An experimental and analytical study on the bending performance of cfrp-reinforced glulam beams,” *Front. Mater.*, vol. 8, p. 802249, 2022. <https://doi.org/10.3389/fmats.2021.802249>
- [15] C. Timbolmas, R. Bravo, F. J. Rescalvo, and A. Gallego, “Development of an analytical model to predict the bending behavior of composite glulam beams in tension and compression,” *J. Build. Eng.*, vol. 45, p. 103471, 2022. <https://doi.org/10.1016/j.jobe.2021.103471>
- [16] X. Zhang, L. Luo, X. Xie, Y. Zhang, and Z. Li, “Flexural bearing capacity and stiffness of stiffened hollow glulam beams: Experiments, fem and calculation theory,” *Constr. Build. Mater.*, vol. 345, no. 4, p. 128407, 2022. <https://doi.org/10.1016/j.conbuildmat.2022.128407>
- [17] A. Buchanan, P. Moss, and W. N., “Ductile moment-resisting connections in glulam beams,” in *Proceedings of NZSEE Conference*, Wairakei Resort, Taupo, New Zealand, 2011. <https://db.nzsee.org.nz/2001/papers/60201paper.pdf>
- [18] A. S. Ribeiro, A. M. de Jesus, A. M. Lima, and J. L. Lousada, “Study of strengthening solutions for glued-laminated wood beams of maritime pine wood,” *Constr. Build. Mater.*, vol. 23, no. 8, pp. 2738–2745, 2009. <https://doi.org/10.1016/j.conbuildmat.2009.02.042>
- [19] R. H. Falk and F. Colling, “Laminating effects in glued-laminated timber beams,” *J. Struct. Eng.*, vol. 121, no. 12, pp. 1857–1863, 1995. [https://doi.org/10.1061/\(ASCE\)0733-9445\(1995\)121:12\(1857\)](https://doi.org/10.1061/(ASCE)0733-9445(1995)121:12(1857))
- [20] H. Yang, W. Liu, and X. Ren, “A component method for moment-resistant glulam beam–column connections with glued-in steel rods,” *Eng. Struct.*, vol. 115, pp. 42–54, 2016. <https://doi.org/10.1016/j.engstruct.2016.02.024>
- [21] R. Mark, “Wood-aluminum beams within and beyond the elastic range. part 1: Rectangular sections,” *For. Prod. J.*, vol. 11, no. 10, pp. 477–484, 1961.
- [22] A. Sliker, “Reinforced wood laminated beams,” *For. Prod. J.*, vol. 12, no. 12, pp. 91–96, 1962.
- [23] K. B. Borgin, G. F. Loedolff, and G. R. Saunders, “Laminated wood beams reinforced with steel strips,” *J. Struct. Div., ASCE*, vol. 94, no. ST7, pp. 1681–1705, 1968.
- [24] G. Lantos, “The flexural behavior of steel reinforced laminated timber beams,” *Wood Sci.*, vol. 2, no. 3, pp. 136–143, 1970.
- [25] W. M. Bulleit, L. B. Sandberg, and G. J. Woods, “Steel-reinforced glued laminated timber,” *J. Struct. Eng., ASCE*, vol. 115, no. 2, pp. 433–444, 1989.
- [26] A. Borri and M. Corradi, “Strengthening of timber beams with high strength steel cords,” *Compos. Part B:*

*Eng.*, vol. 42, no. 6, pp. 1480–1491, 2011. <https://doi.org/10.1016/j.compositesb.2011.04.051>

- [27] O. Garzon Barragán and J. Jacob, “Flexural strengthening of glued laminated timber beams with steel and carbon fiber reinforced polymers,” Master’s thesis, Department of Civil and Environmental Engineering, Chalmers University of Technology, 2007.
- [28] A. Borri, M. Corradi, and A. Grazini, “A method for flexural reinforcement of old wood beams with cfsp materials,” *Compos. Part B: Eng.*, vol. 36, no. 2, pp. 143–153, 2005. <https://doi.org/10.1016/j.compositesb.2004.04.013>
- [29] R. F. Lindyberg, “Relam: A nonlinear probabilistic model for the analysis of reinforced glulam beams in bending,” Ph.D. dissertation, University of Maine, 2000.
- [30] R. Lindyberg and H. Dagher, “Relam: Nonlinear probabilistic model for the analysis of reinforced glulam beams in bending,” *J. Struct. Eng.*, vol. 138, no. 6, pp. 777–788, 2011. [https://doi.org/10.1061/\(ASCE\)ST.1943-541X.0000496](https://doi.org/10.1061/(ASCE)ST.1943-541X.0000496)
- [31] T. P. Nowak, J. Jasieńko, and D. Czepizak, “Experimental tests and numerical analysis of historic bent timber elements reinforced with cfsp strips,” *Constr. Build. Mater.*, vol. 40, pp. 197–206, 2013. <https://doi.org/10.1016/j.conbuildmat.2012.09.106>
- [32] K. C. Johns and S. Lacroix, “Composite reinforcement of timber in bending,” *Can. J. Civil. Eng.*, vol. 27, no. 5, pp. 899–906, 2000. <https://doi.org/10.1139/l00-017>
- [33] R. Hernandez, J. Davalos, S. Sonti, Y. Kim, and R. Moody, “Strength and stiffness of reinforced yellow-poplar glued laminated beams,” US Department of Agriculture, Forest Service, Forest Products Laboratory, Madison (Wisc), Tech. Rep. FPL-RP-554, 1997.
- [34] A. R. Jordan, “Wetpreg reinforcement of glulam beams,” Master’s thesis, The Graduate School, University of Maine, 1998.
- [35] F. Micelli, V. Scialpi, and A. La Tegola, “Flexural reinforcement of glulam timber beams and joints with carbon frp rods,” *J. Compos. Constr.*, vol. 9, no. 4, pp. 337–347, 2005. [https://doi.org/10.1061/\(ASCE\)1090-0268\(2005\)9:4\(337\)](https://doi.org/10.1061/(ASCE)1090-0268(2005)9:4(337))
- [36] H. Johnsson, T. Blanksvärd, and A. Carolin, “Glulam members strengthened by carbon fibre reinforcement,” *Mater. Struct.*, vol. 40, no. 1, pp. 47–56, 2007. <https://doi.org/10.1617/s11527-006-9119-7>
- [37] G. M. Raftery and A. M. Harte, “Low-grade glued laminated timber reinforced with frp plate,” *Compos. Part B: Eng.*, vol. 42, no. 4, pp. 724–735, 2011. <https://doi.org/10.1016/j.compositesb.2011.01.029>
- [38] G. M. Raftery and A. M. Harte, “Nonlinear numerical modeling of frp plate reinforced glued laminated timber,” *Compos. Part B: Eng.*, vol. 52, pp. 40–50, 2013. <https://doi.org/10.1016/j.compositesb.2013.03.038>
- [39] G. M. Raftery and C. Whelan, “Low-grade glued laminated timber beams reinforced using improved arrangements of bonded-in gfrp rods,” *Constr. Build. Mater.*, vol. 52, pp. 209–220, 2014. <https://doi.org/10.1016/j.conbuildmat.2013.11.044>
- [40] H. Alhayek and D. Svecova, “Flexural stiffness and strength of gfrp-reinforced timber beams,” *J. Compos. Constr.*, vol. 16, no. 3, pp. 245–252, 2012. [https://doi.org/10.1061/\(ASCE\)CC.1943-5614.0000261](https://doi.org/10.1061/(ASCE)CC.1943-5614.0000261)
- [41] C. Gentile, D. Svecova, and S. Rizkalla, “Timber beams strengthened with gfrp bars: development and applications,” *J. Compos. Constr.*, vol. 6, no. 1, pp. 11–20, 2002. [https://doi.org/10.1061/\(ASCE\)1090-0268\(2002\)6:1\(11\)](https://doi.org/10.1061/(ASCE)1090-0268(2002)6:1(11))
- [42] C. Gentile, “Flexural strengthening of timber bridge beams using frp,” Master’s thesis, Department of Civil & Geological Engineering, University of Manitoba, 2000.
- [43] A. Borri, M. Corradi, and E. Speranzini, “Reinforcement of wood with natural fibers,” *Compos. Part B: Eng.*, vol. 53, pp. 1–8, 2013. <https://doi.org/10.1016/j.compositesb.2013.04.039>
- [44] E. Speranzini and S. Tralascia, “Engineered lumber: Lvl and solid wood reinforced with natural fibres,” in *World Conference on Timber Engineering (WCTE 2010)*, Riva del Garda, Italy, 2010, paper 798.
- [45] E. Speranzini and S. Agnetti, “Structural performance of natural fibers reinforced timber beams,” in *Proceeding of the 6th International Conference on FRP Composites in Civil Engineering (CICE 2012)*, Rome, Italy, 2012.
- [46] B. Gallant, “Development of a new natural frp composite and its application in glulam tudor arches,” Master’s thesis, Department of Civil Engineering, Dalhousie University, 2004.
- [47] B. Bohannan, “Pre-stressed wood members,” *Forest Prod. J.*, vol. 12, no. 12, pp. 596–602, 1962.
- [48] E. McConnell, D. McPolin, and S. Taylor, “Post-tensioning of glulam timber with steel tendons,” *Constr. Build. Mater.*, vol. 73, pp. 426–433, 2014. <https://doi.org/10.1016/j.conbuildmat.2014.09.079>
- [49] Z. Guan, P. Rodd, and D. Pope, “Study of glulam beams pre-stressed with pultruded grp,” *Comput. Struct.*, vol. 83, no. 28-30, pp. 2476–2487, 2005. <https://doi.org/10.1016/j.compstruc.2005.03.021>
- [50] J. F. Brady and A. M. Harte, “Pre-stressed frp flexural strengthening of softwood gluelaminated timber beams,” in *Proceedings of the 9th World Conference on Timber Engineering, WCTE 2008*, Miyazaki, Japan, 2008.

- [51] M. P. Persson and S. Wogelberg, “Analytical models of pre-stressed and reinforced glulam beams, a competitive analysis of strengthened glulam beams,” Master’s thesis, Department of Civil and Environmental Engineering, Chalmers University of Technology, 2011.
- [52] V. De Luca and C. Marano, “Pre-stressed glulam timbers reinforced with steel bars,” *Constr. Build. Mater.*, vol. 30, pp. 206–217, 2012. <https://doi.org/10.1016/j.conbuildmat.2011.11.016>
- [53] H. Al-Hayek and D. Svecova, “Flexural strength of post tensioned timber beams,” *J. Compos. Constr.*, vol. 18, no. 2, p. 04013036, 2014. [http://doi.org/10.1061/\(ASCE\)CC.1943-5614.0000431](http://doi.org/10.1061/(ASCE)CC.1943-5614.0000431)
- [54] J. H. Negrão, “Preliminary study on wire pre-stressing methods for timber pieces reinforcement,” *Constr. Build. Mater.*, vol. 102, pp. 1093–1100, 2016. <http://doi.org/10.1016/j.conbuildmat.2014.11.050>
- [55] S. Kilincarslan and Y. S. Turker, “Experimental investigation of the rotational behaviour of glulam column-beam joints reinforced with fiber reinforced polymer composites,” *Compos. Struct.*, vol. 262, p. 113612, 2021. <https://doi.org/10.1016/j.compstruct.2021.113612>

## Nomenclature

<i>E</i>	modulus of elasticity, N/mm <sup>2</sup>
<i>F</i>	difference of applied forces, N
<i>L<sub>s</sub></i>	spacing between support points, mm
<i>b</i>	the width of the test sample, mm
<i>h</i>	height of the test specimen, mm
<i>f</i>	displacement amount mm
Ge	flexural strength, N/mm <sup>2</sup>
Fmax	for maximum load at break